AN INVESTIGATION OF THE MAGNETIC APPLICATIONS OF SUPERCONDUCTING CERAMIC MATERIALS.

Miguel Ángel Sáez Paguay [a]*, María Fernanda Heredia Moyano [b], Freddy Patricio Ajila Zaquinaula [c], Rolando Marcel Torres Castillo [c]

[a] Facultad de Recursos Naturales, Escuela Superior Politécnica de Chimborazo (ESPOCH), Orellana 220201, Ecuador

[b] Facultad de Ciencias, Escuela Superior Politécnica de Chimborazo (ESPOCH), Riobamba, 060155, Ecuador

[c] Escuela Superior Politécnica de Chimborazo, Sede Orellana, El Coca, 220001, Ecuador

Abstract

Superconducting ceramic materials have unique electrical and magnetic properties that make them suitable for a wide range of applications, including high-field magnets, microwave filters, and magnetic resonance imaging (MRI) systems. In this paper, we review recent developments in the field of superconducting ceramic materials and their potential use in magnetic applications. The discovery of high critical temperature superconducting (SAT) ceramic materials with $T\_c \approx 100$ K has opened new perspectives for the application of superconductivity in many areas, including electronics. By moving the operating temperature from the liquid helium to the nitrogen range, cooling costs are reduced by several orders of magnitude. Despite the granular nature and other specific problems of SATs, and only five years after their discovery, superconducting wires and devices based on thin films are a reality. In this paper, we review the status of large and small-scale applications for SATs.

Keywords: Ceramic materials; superconductors; medical applications; technological advances; magnetism.

Introduction

Superconducting ceramics, also known as high-temperature superconductors (HTS), are a class of materials that exhibit zero electrical resistance and perfect diamagnetism at temperatures above the boiling point of liquid nitrogen (77 ºK). This makes them attractive for a variety of applications, such as high-field magnets, microwave filters, and magnetic resonance imaging (MRI) systems.

The discovery of superconducting materials at temperatures higher than liquid nitrogen has been one of the most important scientific achievements of the last decade. Although there is still no general theory to explain their appearance and key experiments to guide the theory are lacking, the existing body of results allows us to affirm that they are type II superconductors with high anisotropy and with convential superconducting carriers (Cooper pairs). Some researchers have published results that would indicate the existence of superconducting phases at near-ambient temperatures; however, these results have never been reproducible at temperatures above 110 ºK.

The most important advantage of high-critical-temperature superconductors (HTS) is the need for liquid nitrogen instead of liquid helium, which reduces cooling costs by more than four orders of magnitude [1]. The application potential of these materials in electrical and electronic technology is therefore very high. However, their nature (quaternary ceramic oxides) is requiring major materials engineering efforts before mass production for power applications, or thin films for electronic device applications can be achieved. applications in electronic devices.

The applications under consideration are mostly a continuation of those developed with classical superconductors. Probably the most immediate are small-scale ones: electromagnetic shielding; voltage standards; SQUID sensors; infrared sensors; microwave devices and analogy signal processing. In the longer term, large-scale applications are considered such as microwave cavities; power transmission lines; superconducting magnets; superconducting motors and levitating vehicles; and in the field of electronics superconducting computers.

In this paper, after a summary of the basic properties of technological interest of superconducting materials in general, and those specific to HTS. This research paper presents a review of the current prospects for large-scale applications and some of the most recent results in the field of small-scale applications.

Material properties superconductors.
Zero resistance and critical temperature.
In 1911, Kamerlingh Onnes observed that the electrical resistance of Hg became undetectable below 4.2 °K (see Figure 1) and discovered superconductivity: Below a certain temperature. Below a certain temperature, called the critical temperature, current can flow through the material without loss of power.
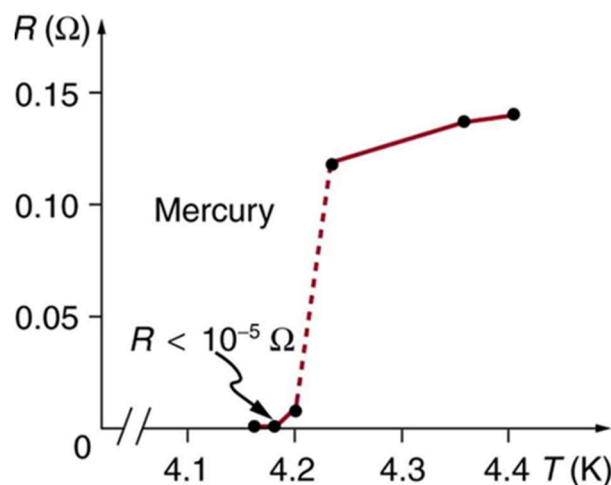
**Figure 1.** Resistance versus temperature of Hg obtained by Kamerlingh Onnes in 1911
He immediately began a search for materials with a superconducting phase and since then, it has been observed in many metals and alloys. Milestones in this development were: 1) The discovery

of superconductivity in Nb (1930) with $T_c = 9.2$ °K (the highest in a pure element). 2) In 1973 a superconducting Nb-Ge alloy was obtained with $T_c = 23.3$ °K (the highest in metals and alloys). 3) Bednorz and Müller (1986) revolutionized the field of superconductivity by detecting superconducting properties in Ba-La-Cu-O metal oxides (ceramic materials) above the 23.3 °K barrier [2]. 4) In early 1987, ceramics of the Y-Ba-Cu-O family gave T_c values above the temperature of liquid nitrogen [3–5], which revolutionized the community scientific-technical community awakening old dreams of applications.

A general rule of thumb in the development of superconductor applications is that the working temperature should be equal to or below $3/4T_c$ [6,7]. Below this temperature, the remaining properties of technological interest, such as the critical magnetic field or the critical current, have values in the order of 1/2 and 1/4 of the low-temperature limit respectively, which are acceptable from an applied point of view. Taking this into account, for a superconducting material to be applicable at liquid nitrogen temperature, $T_c \approx 100$ °K is sufficient. For applications at room temperature it will be necessary to reach $T_c \approx 400$ °K.

2.1. *Meissner effect, critical currents, and fields*

When a superconductor is cooled below Tc, in the presence of a magnetic field, magnetic flux is expelled from its interior (see Figure 2), which in honor of its discoverer (1933) is called the Meissner effect. In turn, if a magnetic field is applied to a superconducting material after cooling it below Tc, it does not penetrate the interior. While flux exclusion would also be present in a perfect conductor, flux ejection, or the Meissner effect, is a unique property of superconductors.
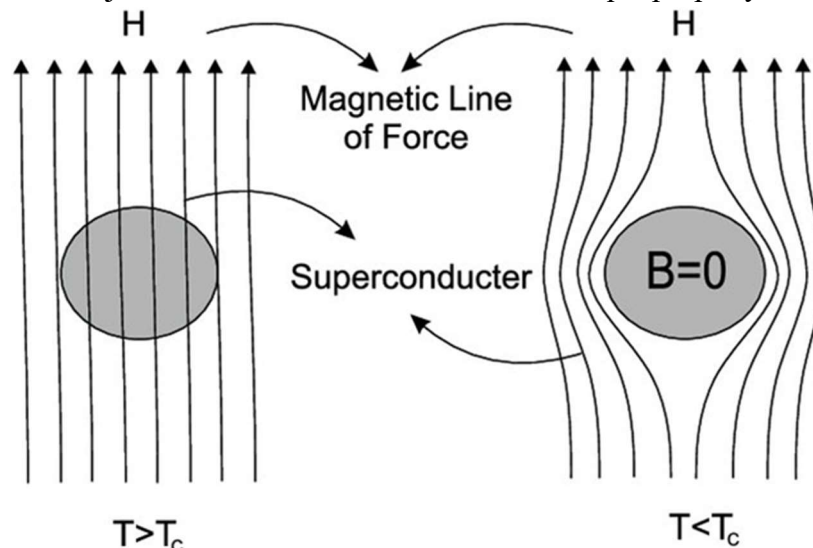
Figure 2. Schematic representation of the Meissner effect of a superconducting material when cooled below T_c in the presence of an applied field $H_a = H_0$ [8].

Depending on their behavior against magnetic fields, superconducting materials are classified into so-called type I and type II materials. type I and type II. Type I materials have a Meissner effect for magnetic fields below a critical value. magnetic fields below a critical value $H_c(T)$, $T < T_c$

while at higher fields the material ceases to be superconducting. Type I superconductors have few practical applications since the critical fields are low (a few hundred Oe).

In contrast, type II superconductors show Meissner effect up to values below a lower critical field H_{c1}. Above H_{c1} the material is no longer homogeneous, allows magnetic flux to enter, and remains partially superconducting up to a higher critical field H_{c2}, which can reach tens of tesla. Between H_{c1} and H_{c2}, the material is in a mixed state with superconducting regions. While the upper critical fields of classical superconducting alloys are between 14 T (Nb-Ti) and 23 T (Nb-Sn), at 4.2 K, the corresponding values for Y-Ba-Cu-O are of the order of 100 T (4). The SATs have revealed the existence of an irreversibility field H_{irr} $H_{c1} < H_{irr} < H_{c2}$ (Figure 3) [9], above which magnetization is reversible, and there is power dissipation when an electric current passes.
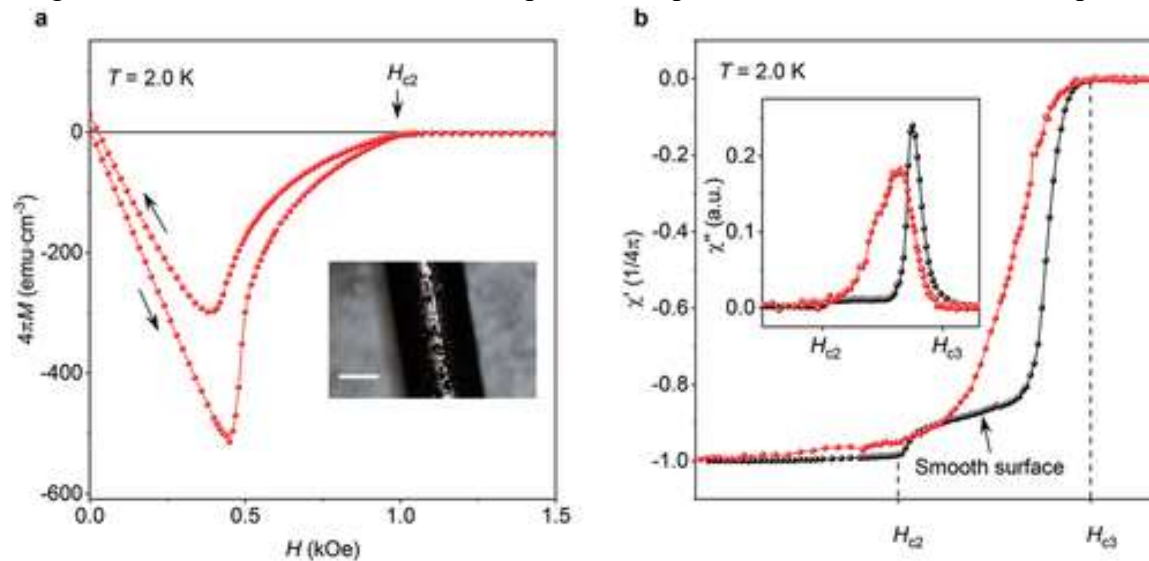

Figure 3. Magnetization curve versus field, $4\pi M(H)$, of a type II superconductor at $T < T_c$. Below H_{c1} the superconductor exhibits Meissner effect $B = 4\pi M + H = 0$. Between H_{c1} and H_{c2} the material is in a mixed state (partial penetration of magnetic flux in the form of flux tubes). Above H_{irr} the flux tubes move freely, so the material does not support electric current. Above H_{c2} the material is in the normal state [10].

For a given temperature and applied field, the maximum current that can flow through the superconducting material is the critical current density J_c. For practical, large-scale applications, values of 10^5 A/cm^2 in the presence of magnetic fields up to 5 T are required. For small-scale applications (microelectronics) the required critical current density is 10^6 A/cm^2 in the absence of a field. The highest values of critical current density, measured inductively, in Y-Ba-Cu-O ceramic materials are 10^4 A/cm^2 at 4.2 K and 6 T, and two to three orders of magnitude lower at 77 K [1,2,5]. In addition, the critical transport currents are lower than the inductive currents due to the granular nature of these materials [11]. Consequently, for practical applications, the grain-to-grain junctions need to be improved.

2.2. *Quantification of magnetic flux.*

When a superconducting ring is cooled in the presence of a magnetic field, the flux is expelled at the instant of magnetic field, at the instant of passing through T_c the flux is expelled from the ring. At the same time the magnetic flux inside the ring is adjusted to a value equal to an integer number of times the flux quantum $\Phi_0 = 2,06x10^{-15} * Tm^2$.Furthermore, if the applied magnetic field is removed, the flux inside the ring does not change (Figure 4). Φ_0 is an extremely small quantity (the earth's magnetic field, which is of the order of 0.4 Oe, produces, in a loop of 1 cm^2, a flux of $2x10^6\Phi_0$).
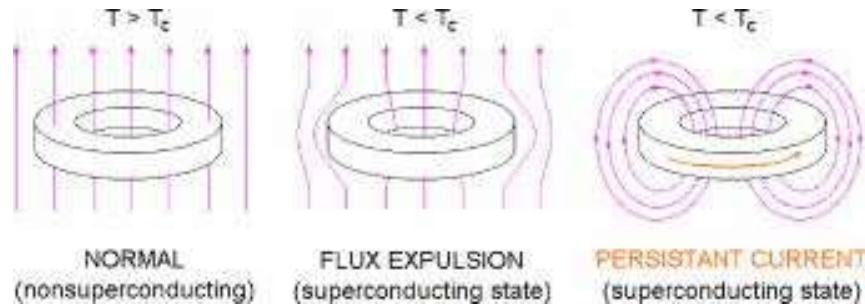

Figure 4. Schematic representation of the quantification of the magnetic flux in a superconducting ring when it is cooled below t_c in the presence of an applied field $H_a = H_0$. Even if H_a is removed, the flux inside the inside the ring does not change [12].

2.3. *Josephson effect.*

If two superconductors are joined through a "weak junction" (insulating barrier, point contact, etc.) (Figure 5a) the assembly can behave as a superconductor due to the tunneling effect in the passage of electron pairs through the junction. This effect was discovered by Brian Josephson in 1962 [13]. The I-V characteristics of Josephson junctions [14] allow the fabrication of high switching speed logic gates, of great interest in the field of microelectronics. However, the development of computers based on low-temperature superconducting devices has not prospered.

The combination of the properties of superconducting rings and Josephson junctions has resulted in superconducting quantum interference devices (SQUIDs) (Figure 5b) that are the most sensitive magnetic field sensors today [15–19]. SQUID detectors based on classical superconductors are applied in biomedicine, basic research, design of low-noise measurement instrumentation, etc., and can be purchased commercially.
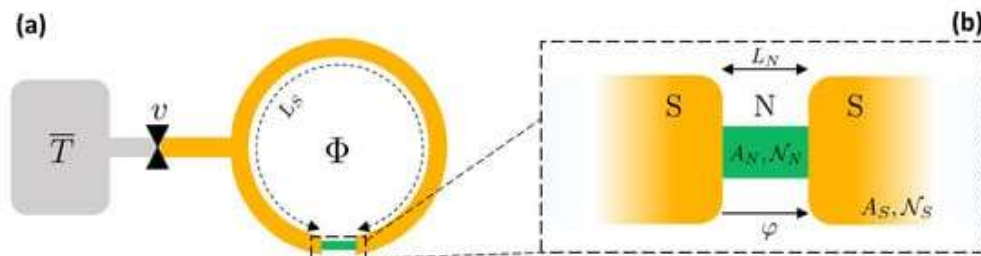
Figure 5. a) Josephson junction formed by two superconductors joined by an insulating material or normal conductor b) "Superconducting Quantum Interference Superconducting Device (SQUID)" formed by a superconducting ring containing a Josephson junction [20].

3. Specific properties of SAT.

3.1. *Anisotropy.*

Three families of materials have been discovered so far SAT with $T_c > 77K$: 1) M-Ba-Cu-O, where M=Y, Nd, La, Sm, Eu, Gd, Dy, Ho, Er, Tm, Yb, Lu, with $T_c \approx 85 - 95$ K. 2) Bi-SrCa-Cu-O, with $T_c \approx 85 - 110K$ 3) Tl-Ca-Ba-Cu-O with $T_c \approx 120K$ [21]. SATs were first synthesized in the form of ceramic materials with grains of varying size and orientation. Critical currents of 1 to 10^3 A/cm^2 and lower critical fields of a few Oe were determined by the weak contacts between the randomly oriented crystals rather than by intrinsic properties [22]. This made the practical application of these superconductors unthinkable. Fortunately, oriented bulk materials with good inter-grain contacts and epitaxially grown thin films, which exhibit sufficient critical currents for first applications, have now been prepared.

Table 1 presents the values of T_c, coherence length ξ, penetration length λ, and Ginzburg-Landau critical current density j$_{GL}$, of YBa$_2$ Cu$_3$ O$_{7-\delta}$ in the ab planes and in the c direction at 77 K. By comparison the values for Nb at 4.2 K are also given. The highest values of critical current density obtained experimentally in thin films are two orders of magnitude lower than j$_{GL}$, possibly due to surface defects [1].

Table 1. Basic parameters of a SAT (YBa$_2$ Cu$_3$ O$_{7-\delta}$ at 77K), S. Those of a classical superconductor (Nb at 4.2 K)

Material and Direction	T_c (K)	ξ (T) (nm)	λ (T) (nm)	j$_{GL}$ (T) (A/cm^2)
Y-Ba-Cu-O (ll ab)	95	7	50	5x10^8
Y-Ba-Cu-O (_l_ab)	95	1,5	250	1x10^8
Nb	9,25	40	40	5x10^7

3.2. *Mechanical properties*

TSS are hard but very fragile. Therefore, the manufacture of superconducting wires presents great difficulties. One of the techniques being used is the manufacture of wires by extrusion of ceramic powders in Ag and Cu tubes or oriented fibers. Since it is the last oxidation heat treatment that imparts brittleness to the ceramic material, it must be applied after winding. For the fabrication of parts in applications such as RF cavities, known techniques for machining ceramic materials can be used. The study of the adhesion of TSS with other materials (substrates), resistance to thermal cycling, etc., is essential for microelectronics applications.

3.3. *Chemical stability.*

Both water and carbon dioxide degrade SAT at room temperature, with the formation of hydroxides and carbonates. Oxygen, on the other hand, readily leaves the structure in a vacuum and at room temperature. Therefore, surface protection techniques have to be applied, especially for thin films.

3.4. *Radiation effects.*

In certain applications such as magnetic fusion, the radiation sensitivity of the materials used is extremely important. SATs are more sensitive to radiation than classical superconductors, but several orders of magnitude less so than semiconductors, making them very interesting for electronic applications.

3.5. *Losses in alternating current.*

Conventional superconductors have AC losses that affect applications such as 50 Hz power transmission lines or microwave devices. In SAT, losses are essentially due to magnetic hysteresis phenomena [23] and are substantially reduced by improving the inter-grain junctions and the degree of orientation. and the degree of orientation.

4. Large-scale applications

4.1. *High and/or very stable field coils.*

Classical superconductors (Nb-Ti, Nb-Sn) have been used to produce superconducting coils for scientific applications (physical measurements in intense fields up to 20 T, nuclear fusion), medical (NMR imaging with very stable 1.5 T coils) and industrial applications (magnetic separation in mines and industrial plants, high power-to-weight ratio motors). The manufacture of SAT coils requires the production of high quality multi-stranded wires. These could replace classical coils in some scientific and industrial applications, where the main cost is the system where the main cost is the magnetic field generation system. However, in complex medical MRI systems they will not be competitive in the medium term, given the high cost of the rest of the instrumentation. In spite of the enormous technical difficulties involved in SATs when manufacturing flexible cable with high critical current, and only five years after their discovery, promising results have already been achieved.

Thus, General Atomics Company has produced SAT (Rare Earth-Ba-Cu-O) fibers of 1000m in length and 0.3mm in diameter in Cu matrix [24,25]. These fibers have been used to produce up to 20 m of 0.9mmx5,7 mm superconducting cable with a cross-section of 12 strands. The critical current at zero field and 50 K is greater than 10 A, which corresponds to critical current densities of 5000 A/cm^2. This is reduced by a factor of 10 under fields of a few tenths of a tesla. With the cable, 15cm diameter coils can be constructed without reducing the critical current. The company's forecast for the end of 1991 is to manufacture kilometers of multifilamentary cable with critical current densities of $2x10^3$ A/cm^2.

The Sumitomo Company has fabricated Bi-Sr-Ca-Cu-O (2:2:2:3) wire by extrusion of ceramic powder in Ag tube [26,27]. With it, it has built a coil capable of generating a magnetic field of 1 T at 4.2 K. He is currently fabricating a triple solenoidal coil consisting of an external Nb-Ti coil, an intermediate Nb-Sn coil and an intermediate Nb-Sn coil. Nb-Sn intermediate coil and the innermost SAT coil. Due to the high critical field of the SAT material the inner coil can generate 0.25 T in the presence of 23 T generated by the outer ones. The result is a 23.25 T coil. The few

tenths added by the SAT coil will make it possible to reach frequencies of 1 GHz in NMR equipment. GHz in NMR equipment.

4.2.*Transmission lines and power devices.*

The Westinghouse Company in collaboration with Argonne have developed a power transmission line 64 cm long and 7,4cm in diameter, which uses 17 rectangular SAT bars made of a composite of Y-Ba-Cu-O and Ag [28]. The line can carry 2000 A (250 A/cm^2) and withstands a maximum magnetic field of 0,18 T. By using these SAT connections in the low-temperature parts of superconducting power devices, He evaporation can be reduced by 40%. SAT connections are important in space applications, where liquid helium evaporation limits the lifetime of devices. For its part, Argonne has built the first experimental SAT-based motor operating in liquid nitrogen, capable of rotating at 50 cycles per minute [3,4].

4.3. Magnetic levitation.

The fabrication of SAT by the Melt-Powder-Melt-Growth (MPMG) method has made it possible to increase the grain size and improve the bonds between grains and their degree of orientation. The materials obtained by this method show critical intergranular currents similar to the intragranular ones and of the order of 10^4 A/cm^2 at 77 K. The magnetic field penetrates the superconductor with a $\frac{dB}{dx}$ gradient proportional to J_c, so the maximum force of levitation force is proportional to J_c and to the volume of superconducting material. This explains the spectacular magnetic levitation experiments of permanent magnets on SAT produced by the MPMG method. Thus, the Superconductivity Research Laboratory (ISTEC, Tokyo), has succeeded in levitating a total of 120 kg, supported by a permanent magnet producing a magnetic field of 2,5 T, on a set of 250 Y-Ba-Cu-O pellets, each 3cm in diameter and 1,5 cm thick, cooled with liquid nitrogen [7,9]. SAT-based levitation vehicles may become a long-term reality. be a reality in the long term.

4.4. Medical applications

ICI Advanced Materials Company has developed Y-Ba-Cu-O coils that have been used, immersed in liquid nitrogen, as collector coils for a 0.15 T NMR scanning machine at Hammersmith Hospital in London [3,13,20]. The first MRI image of a human brain using SAT has been obtained with these coils. The SAT coil has higher sensitivity than the usual Cu coils, giving a higher signal-to-noise ratio. This reduces the number of scans needed to obtain an image, and therefore the costs.

5. Small-scale applications.

applications, especially in electronics, then in large-scale applications. As in the latter, it is necessary to solve the problems associated with the specific properties of TSS mentioned above, but in this case, it is also necessary to consider, for each specific application, the influence of the increase in thermal fluctuations in temperature. The step from 4 K to 77 K means an increase of a factor of 20 in thermal fluctuations. This factor is especially important in devices containing Josephson junctions. In this case the fluctuations can be characterized by a dimensionless factor given by the expression [29]:

$$\gamma \equiv \frac{2\pi k_B T}{\Phi_0 I_c} \equiv \frac{I_T}{I_c}, \qquad I_T \equiv \frac{2\pi k_B T}{\Phi_0}$$

In most devices and must not exceed certain limits (between 10^{-3} and 10^{-1}), so that the critical junction current I_c is always considerably larger than the "thermal current" I_T. For T=4.2 KI_T is very small ($\approx 0,2$uA) so that the condition $I_c > I_T/\gamma_{max}$ is easily met. For t$\approx$77 K, $I_T \approx 3,2$uA, so the required I_c values must be greater than 3 mA. Such high critical current values cause two major problems:

1) *The power dissipated by a junction is given by the expression.*

$$P = \overline{IV}\alpha I_c \overline{V}$$

and therefore, grows proportionally to T (for fixed γ and V). In addition, some superconducting devices rely on the rapid growth of the quasiparticle current occurring at the voltage associated with the junction barrier, V_g. Since

$$\overline{V} \approx V_g \equiv \frac{2\Delta(T)}{e}$$

where Δ(T) is the energy barrier of the superconductor which, according to BCS theory, is proportional to T_C, the dissipated power is proportional to T^2. This huge increase is prohibitive in superconducting LSI circuits. superconductor circuits.

*2) Many of the Josephson devices are SQUIDs. Their basic parameter* [29]*:*

$$I = \frac{2\pi L I_c}{\Phi_0}$$

must be of the order of 3 for proper operation, so that the inductance of the superconducting ring, L, is proportional to T^{-1} for y constant. For example, at T=77 K and $\gamma = 10^{-3}$, the result is I_c=3 mA and L=0.3 pH. The only way to build such small inductances is by means of structures formed by superconducting microlines, which will be very difficult even in the medium term. Therefore, with SAT it will be necessary to work with higher values of γ that allow lower values of I_c and higher L, even at the cost of deteriorating the signal-to-signal ratio. at the cost of deteriorating the signal-to-noise ratio.

5.1. Josephson Unions

Josephson junctions are the basic active elements of superconductor-based electronics. The standard theory of superconductivity states that the maximum switching frequency of an S-N-S junction is given by the maximum value of the characteristic frequency of the ω_c junction and this is:

$$(\omega_c)_{max} \approx 15\frac{k_B}{h}\left(T_c(T_c - T)\right)^{\frac{1}{2}} \quad para\ T \leq T_c$$
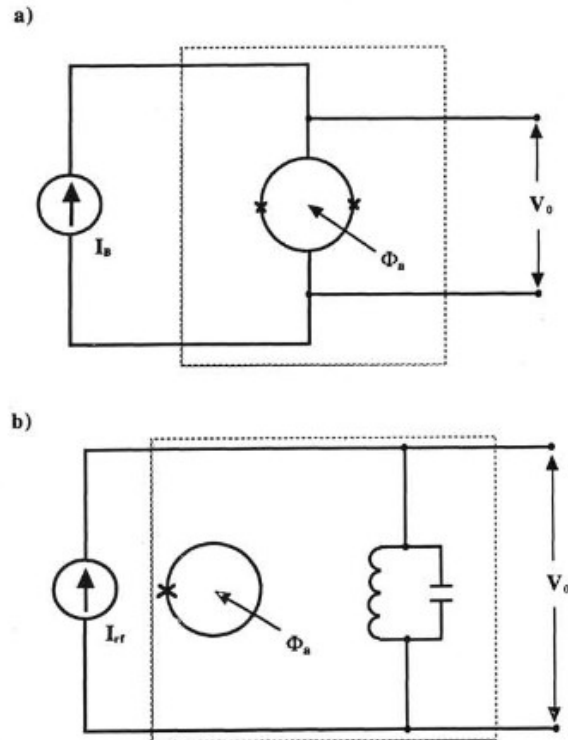
Figure 6. Schematic representation of: a) a SQUID with two Josephson junctions (X-X), and b) a SQUID rf with one junction. Bias circuits have been included. V_0 is the output voltage and is urm periodic function of the applied flux Φ_a with period Φ_0. The dashed regions are at low temperature.

For the 1-2-3 phase with $T_c = 95K$ the expected value at 77 K is $(\omega_c)_{max} = 3x10^{13}s^{-1}$. S-N-S junctions exist naturally on SAT and can be isolated by simply choking the material to the same size as the grains (18). But they are not reproducible, which makes their controlled fabrication in devices difficult. Tunnel junctions (S-I-S) are easier to construct reproducibly. But in this case, it is the plasma frequency œ^ that limits the switching time. This depends directly on the critical current and with the present values, at 77 K can be obtained $\omega_P = 10^{12}s^{-1}$. These values are of the order of those achieved with the best junctions fabricated with classical superconductors.

5.2. SAT-based SQUID sensors.

A SQUID is a flow-to-voltage transducer. Physically it consists of a ring of superconducting material whose size can range from a few millimeters to several mm. There are two classes of SQUIDs: de SQUIDs and rf SQUIDs where de and rf refer to the type of excitation needed to bias the device. The de SQUID has two Josephson junctions and the rf SQUID has only one [15,21,22].
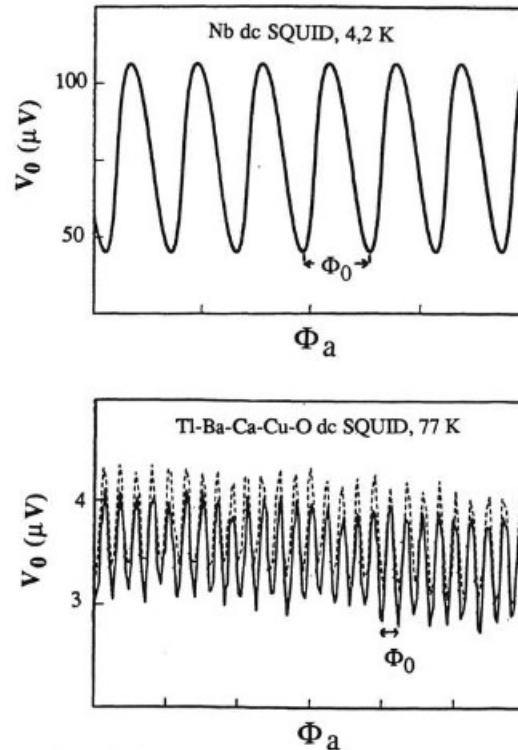
Figure 7. Graphical representation $V_0(\Phi_0)$ of a SQUID of Nb operating at 4y2 K. b) Graphical representation$V_0(\Phi_0)$ SQUID of de Tl$_2$Ba$_2$Cu$_2$O$_y$ operating at 77 K.

The SQUID dc works in a simple way. A higher than critical bias current is applied to the device and a voltage is obtained at its ends (Figure 6a). This voltage, due to flux quantization inside the superconducting ring, depends periodically on the magnetic flux passing through the SQUID, the period being Φ_0 (figure 7). In the case of a rf SQUID, a bias rf current is applied in an LC circuit inductively coupled with the SQUID. inductively coupled with the SQUID. The rf voltage sensed in the LC circuit varies periodically with the flux in a manner similar to that in figure 7.

SQUID sensors alone are not particularly sensitive to the magnetic field due to their small size. To increase their sensitivity, flux transformers are used. These consist of two superconducting coils interconnected to form a closed circuit. The collector coil (several cm in diameter) transforms the flux that passes through it and that is to be measured into a current that flows through the input coil, which is smaller and inductively coupled to the SQUID. This creates a magnetic field in the SQUID of higher intensity than the one existing in the pick-up coil. Flux transformers are manufactured with superconducting wire or by means of superconductor wire or by means of thin film technology (planar coils). The sensitivity of SQUID detectors, built with classical superconductors, ranges from 10^{-4} Φ_0/Hz for rf to 10^{-5} Φ_0/Hz$^{1/2}$ for dc. They can be used to build magnetometers with sensitivities down to 0.01 pT/Hz$^{1/2}$. The sensitivity of SQUIDs made with SAT can approach that of low-temperature ones if $\gamma <0,1$ is made which implies I_c>30 mA and L <30pH.

Recently, a group of researchers from Berkeley (California) has published the fabrication of a magnetometer based on a SAT SQUID [30,31]. Both the SQUID device and the flux transformer have been constructed with thin film technology using $YBa_2Cu_3O_{7-g}$ as superconducting material. The sensitivity of the magnetometer is $0,35 \ pT/Hz^{1/2}$. Electrocardiograms in humans have been performed with it, obtaining results similar to those obtained with low-temperature SQUID magnetometers (Figure 8).

5.3. Voltage patterns

When a Josephson junction is irradiated with radiofrequency the I-V curve presents, in addition to the current step at zero voltage (corresponding to the critical current), current steps at well-defined voltage values that depend on fundamental constants and the frequency of radiation. This fact has been used for the fabrication of voltage standards [32]. Current devices based on classical superconductors consist of thousands of series junctions with which voltage steps of up to 10 V are achieved, making the rest of the instrumentation for comparison with the secondary pattern relatively simple. The current steps have been observed in weak SAT junctions [33] which allows us to venture the achievement of primary voltage standards fainting at 77 K in the medium term.

5.4. Electromagnetic shielding.

The large reduction in cooling costs justifies applications that were not cost-effective with conventional superconductors. Thus, magnetic shielding with superconductors, a conceptually simple application, has been restricted to systems using liquid helium for other reasons. Thanks to the Meissner effect, a superconducting layer of thickness d of the order of several times the penetration length $\lambda(T)$, produces virtually perfect shielding for all frequencies from dc to beyond the ultraviolet. At low frequencies, the most unfavorable case, the critical power, p_c, which a superconductor is capable of shielding, is proportional to H_{c1}^2. for the single-crystalline 1-2-3 phase with the shielding surface parallel to the plane ab, $H_{c1} = 100 \ Oe$ and $Pc = 10^6 \ W/cm^2$, more than sufficient in most cases. SAT electromagnetic screens are commercially available [30,31].

Conclusions

In conclusion, superconducting ceramic materials have unique electrical and magnetic properties that make them suitable for a wide range of applications, including high-field magnets, microwave filters, and magnetic resonance imaging (MRI) systems. Further research is needed to improve the performance of these materials and to develop new applications.

SAT materials have specific properties (granularity, anisotropy, etc.) that make the manufacture of cables and devices extremely difficult. However, the use of liquid nitrogen instead of liquid helium greatly reduces costs and simplifies the design and operation of applications. This has meant that research centers around the world and industries with expertise in superconductivity are devoting a great deal of effort to the rapid resolution of TSS problems. The result is encouraging, since, in just five years, it has been possible to produce wires and devices that, although not optimized, offer promising application prospects. In fact, high critical field

superconducting coils and magneto cardiograms with SQUIDs made of SAT material are already a reality. SAT material are already a reality.

Acknowledgments

References

[1]   K.K. Likharev, V.K. Semenov, A.B. Zorin, New possibilities for superconductor devices, in: Supercond. Devices, Academic Press New York, 1990: pp. 1–49.

[2]   J.G. Bednorz, K.A. Müller, Possible high T c superconductivity in the Ba− La− Cu− O system, Zeitschrift Für Phys. B Condens. Matter. 64 (1986) 189–193.

[3]   A.A. El-Hamalaway, The role of Y/Ba on the formation of high-T c superconducting phase in Y-based system, J. Supercond. 6 (1993) 305–311.

[4]   M.T. Anderson, K.R. Poeppelmeier, Structural similarities among cuprate superconductors, Appl. Supercond. 1 (1993) 493–502.

[5]   A. Amoretti, Condensed matter applications of AdS/CFT: Focusing on strange metals, Springer, 2017.

[6]   V.D. Hunt, Superconductivity sourcebook, (1989).

[7]   Y. Grigorashvili, Superconductors: Properties, Technology, and Applications, BoD–Books on Demand, 2012.

[8]   J. Balasubramanyam, S. Thomas, Lecture Notes on Engineering Physics, (2014).

[9]   K.A. Miller, M. Takashige, J.G. Bednorz, Flux trapping and superconductive glass state in La2Cu04_y: Ba, Phys. Rev. Lett. 58 (1987) 1143–1146.

[10]   W. Kuang, G. Lopez-Polin, H. Lee, F. Guinea, G. Whitehead, I. Timokhin, A.I. Berdyugin, R.K. Kumar, O. V. Yazyev, N. Walet, A. Principi, A.K. Geim, I. V. Grigorieva, Magnetization Signature of Topological Surface States in a Non-Symmorphic Superconductor, Adv. Mater. 33 (2021) 1–8. https://doi.org/10.1002/adma.202103257.

[11]   D.C. Larbalestier, S.E. Babcock, X. Cai, M. Daeumling, D.P. Hampshire, T.F. Kelly, L.A. Lavanier, P.J. Lee, J. Seuntjens, Weak links and the poor transport critical currents of the 123 compounds, Phys. C Supercond. 153 (1988) 1580–1585.

[12]   R.L. Fagaly, Superconducting quantum interference device instruments and applications, Rev. Sci. Instrum. 77 (2006). https://doi.org/10.1063/1.2354545.

[13]   B.D. Josephson, Possible new effects in superconductive tunnelling, Phys. Lett. 1 (1962) 251–253.

[14]   A. Barone, G. Paterno, Physics and applications of the Josephson effect, Wiley Online Library, 1982.

[15]   J.C. Gallop, SQUIDs, the Josephson effects and superconducting electronics, CRC Press, 2017.

[16] I. Askerzade, A. Bozbey, M. Cantürk, Modern aspects of Josephson dynamics and superconductivity electronics, Springer, 2017.

[17] F. Tafuri, Fundamentals and frontiers of the Josephson effect, Springer Nature, 2019.

[18] A.F. Volkov, P.H.C. Magnée, B.J. Van Wees, T.M. Klapwijk, Proximity and Josephson effects in superconductor-two-dimensional electron gas planar junctions, Phys. C Supercond. 242 (1995) 261–266.

[19] Y. Tanaka, S. Kashiwaya, Theory of Josephson effect in superconductor-ferromagnetic-insulator-superconductor junction, Phys. C Supercond. 274 (1997) 357–363.

[20] F. Vischi, M. Carrega, A. Braggio, P. Virtanen, F. Giazotto, Thermodynamics of a phase-driven proximity Josephson junction, Entropy. 21 (2019) 1–33. https://doi.org/10.3390/e21101005.

[21] D.M. Ginsberg, Introduction, history, and overview of high temperature superconductivity, in: Phys. Prop. High Temp. Supercond. I, World Scientific, 1989: pp. 1–38.

[22] M. Tinkham, C.J. Lobb, Physical properties of the new superconductors, in: Solid State Phys., Elsevier, 1989: pp. 91–134.

[23] K.-H. Müller, Detailed theory of the magnetic response of high-temperature ceramic superconductors, Magn. Susceptibility Supercond. Other Spin Syst. (1991) 229–250.

[24] M. Humphries, Rare earth elements: the global supply chain, Diane Publishing, 2010.

[25] J.A. Goldman, The US rare earth industry: its growth and decline, J. Policy Hist. 26 (2014) 139–166.

[26] J.E. Hirsch, Superconductivity, what the H? The emperor has no clothes, ArXiv Prepr. ArXiv2001.09496. (2020).

[27] P. Tixador, Superconducting magnetic energy storage: Status and perspective, in: IEEE/CSC ESAS Eur. Supercond. News Forum, 2008.

[28] A.M. Goldman, Superconductor-insulator transitions, Int. J. Mod. Phys. B. 24 (2010) 4081–4101.

[29] K.K. Likharev, Dynamics of Josephson junctions and circuits, Routledge, 2022.

[30] A.H. Miklich, J.J. Kingston, F.C. Wellstood, J. Clarke, M.S. Colclough, K. Char, G. Zaharchuk, Sensitive YBa2Cu3O7− x thin-film magnetometer, Appl. Phys. Lett. 59 (1991) 988–990.

[31] D. Grundler, B. David, R. Eckart, O. Dössel, Highly sensitive YBa2Cu3O7 dc SQUID magnetometer with thin-film flux transformer, Appl. Phys. Lett. 63 (1993) 2700–2702.

[32] R. Kautz, C. Hamilton, F. Lloyd, Series-array Josephson voltage standards, IEEE Trans. Magn. 23 (1987) 883–890.

[33] D. Robbes, M.L.C. Sing, Y. Monfort, D. Bloyet, J. Provost, B. Raveau, Bulk dc SQUID in a Tl-based ceramic: Shapiro steps, signal, and noise properties at 77 K, Appl. Phys. Lett. 54 (1989) 1172–1174.